J. Water Environ. Nanotechnol., 5(1): 56-67 Winter 2020

ORIGINAL RESEARCH PAPER

Removal of bisphenol A from water solution using molecularly imprinted nanopolymers: Isotherm and kinetic studies

Seyedeh Maedeh Hashemi Orimi[1], Maryam Khavarpour[1,*], Sohrab Kazemi[2]

[1] Department of Chemical Engineering, Ayatollah Amoli Branch, Islamic Azad University, Amol, Iran
[2] Cellular and Molecular Biology Research Center, Babol University of Medical Sciences, Babol, Iran

Received: 2019-10-25 Accepted: 2019-12-07 Published: 2020-02-01

ABSTRACT

In the present study, the adsorption behavior of mesoporous molecularly imprinted polymers for bisphenol A was investigated. Molecularly imprinted nanopolymers were synthesized by precipitation polymerization using bisphenol A as a template molecule. Two molecular ratios of template: functional monomer: cross-linker (1:6:30 (MIP-6) and 1:4:20 (MIP-4)) was considered for experiments. Ethylene Glycol Dimethacrylate (EGDMA) as a Crosslinker, methacrylic acid (MAA) as a functional monomer and 2, 2´-azobisisobutyronitrile (AIBN) as an initiator were used for the synthesis of polymers. Moreover, Langmuir and Freundlich adsorption isotherms, and pseudo-first-order and pseudo-second-order kinetic models were studied for the adsorption mechanism. Results showed that porous polymers with an average pore diameter of 13 to 17 nm and a specific surface area of 326 to 439 (cm^3/g) were obtained. The maximum adsorption capacity was 400.1 µmol/g for MIP-6. SEM analysis showed that the synthesized polymer particles were spherical. The highest adsorption efficiency of bisphenol A achieved by MIP-6 was 71%.

Keywords: *Bisphenol A; Molecularly imprinted polymer; Mesosphere; Isotherm; Kinetic adsorption*

How to cite this article
Hashemi Orimi SM, Khavarpour M, Kazemi S. Removal of bisphenol A from water solution using molecularly imprinted nanopolymers: isotherm and kinetic studies. J. Water Environ. Nanotechnol., 2020; 5(1): 56-67.
DOI: 10.22090/jwent.2020.01.005

INTRODUCTION

Molecularly imprinted polymers as tailor-made adsorbent are used to recognize target molecules. They have a memory of the size, shape, and functionalities complementary to the template molecules [1]. Some polymerization approaches such as bulk polymerization [2], suspension polymerization [3], mini-emulsion polymerization [4], and precipitation polymerization [5] have been developed to synthesize three-dimensional network polymers.

MIPs prepared by bulk polymerization are ground and sieved to obtain a desirable size of particles which may result to destroy the cavities, irregular shape, and reduction in yield of useful size [6].

On the other hand, methods such as suspension polymerization and mini-emulsion polymerization may face difficulties including prolonged optimization of the experimental procedure and existing remained emulsifier or stabilizer on the adsorbent [7]. Thus, precipitation polymerization is preferred because of resulting in the spherical and uniform shape of particles, narrow size distribution, and a surfactant or stabilizer-free polymerization.

MIPs are prepared by the co-polymerization of functional monomers with cross-linkers around template molecules. Interaction of the functional monomers with templates forms a stable complex [8]. After the polymerization process, the template molecules are removed, leading to well-defined and highly cross-linked three-dimensional cavities. The resulting MIPs can rebind the template molecules with high selectivity. They are stable, controllable,

* Corresponding Author Email: *mkhavarpoor@yahoo.com*

and resistant to varying temperatures, pH, and solvent [9]. The nucleation and growth process of MIPs can be adjusted by factors such as functional monomer, porogen, cross-linker, template, and initiator. [10]. Duo to significant advantages of using MIPs including ease and low cost of preparation, MIPs have wide applications such as protein recognition [11], solid-phase extraction [12, 13], sensors [14, 15], environmental [16], drug delivery systems [17] and antibody substitutes [18]. Bisphenol A (BPA) have extensively used in industrial chemical, as a primary raw material and as an intermediate to the production of epoxy resins, polycarbonate plastic, food and drink containers, baby formula bottles, electronic apparatus and medical facilities [19-21]. BPA has a harmful effect on the environment and endocrine systems of humans and animals [22, 23]. Therefore, it is essential to remove BPA in various samples due to its toxic influence.

Several attempts have been made to synthesize MIP by various polymerization to remove BPA from food, water, and milk solution. Hiratsuka et al. (2013) synthesized a magnetic molecularly imprinted polymers (M-MIPs) for BPA detection in river water by a multi-step swelling and polymerization method. He showed that the binding experiments and Scatchard analyses revealed two classes of binding sites [24]. In another study, Alexiadou et al. (2008) prepared MIP for BPA by two synthetic routes: semi-covalent and noncovalent methods. They evaluated the molecular imprinting effect using the polymers in HPLC and SPE. The most critical factors of fabricated MIP were the organic content in loading–washing medium and the washing volume. Moreover, low flow rates in the elution step enhanced extraction recovery [25].

Despite several studies undertaken on BPA removal by MIP, there is rare information on isotherm and kinetic investigation to find out the mechanism of the process. In the present work, the precipitation polymerization is selected for MIP synthesis due to the advantages mentioned earlier. The prepared polymers are characterized by Fourier transform infrared spectroscopy (FTIR) to determine the functional groups. The morphologies and pore size of the obtaining imprinted particles are characterized by scanning electron microscopy (SEM) and Brunauer–Emmett–Teller (BET) gas adsorption measurements, respectively. The effect of molecular ratios of template: functional monomer: cross-linker on adsorbent capacity, BPA removal efficiency, polymer structure, and pore size are evaluated. Furthermore, the mechanism and binding properties of polymers are studied.

EXPERIMENTAL

Materials

Bisphenol A (BPA), ethylene glycol dimethacrylate (EGDMA), Methacrylic acid (MAA), 2, 2´- azobisisobutyronitrile (AIBN) were obtained from Sigma Aldrich (Steinheim, Germany). AIBN was purified by recrystallization from methanol before use. Acetonitrile, acetone, acetic acid, and methanol were HPLC grade, purchased from Merck (Darmstadt, Germany) and used without further purification.

MIP synthesis

The MIPS were synthesized in two molecular ratios of 1:4:20 and 1:6:30 (template: functional monomer: cross-linker) as follows: First, for the synthesis of 1:4:20 polymer, 0.182 g (0.798 mmol) of BPA (template) and 0.35 ml (3.192 mmol) of MAA (functional monomer) were dissolved in 15 ml of the porogen acetone. The solution was stirred for 10 min. Then, 3 ml (15.96 mmol) of EGDMA as cross-linker and 50 mg (0.304 mmol) of AIBN as initiator were added to the previous solution. The pre-polymerization solution was sonicated for 10 min at room temperature and purged with nitrogen for 15 min in ice-bath to remove dissolved oxygen. The reaction was performed at 60 °C in a water bath for 24 h to achieve a solid polymer. For the synthesis of 1:6:30 polymer, the amounts of functional monomer and cross-linker were 6 and 30 folds of template amount, respectively. Non-imprinted polymers (NIPs) were synthesized exactly by the similar procedure of MIPs without bisphenol A [26].

Template removal from MIPs

To remove the template, the prepared polymers were transferred into a flask containing methanol/acetic acid (9:1 V/V) and the solution was continuously stirred with a magnetic stirrer during the extraction. The extraction was continued until the absorbance of the filtered solution at 278 nm reached to zero. Then, the template -free MIPs have separated from the solution by centrifuge 10000 rpm, washed with distilled water, and dried at oven at 50 °C overnight. For NIPs, Soxhlet extraction was omitted.

Preparation of BPA calibration plot

To prepare the BPA calibration plot, different concentrations of BPA were made in the acetonitrile solvent. The absorption of the samples was measured at a wavelength of 278 nm and the standard absorption plot and the corresponding equation were obtained. The achieved calibration plot is shown in Fig. 1.

Characterization of MIPs and NIPs

The scanning electron microscope (SEM) (TESCAN, VEGALL, Czech) was used for the estimation of the shape and surface morphology of the polymers. Polymeric particles were sputter-coated with gold before the SEM measurement. Nitrogen adsorption-desorption measurements were performed based on adsorption or desorption of nitrogen on or from polymer surface at 77K using BELSORP measuring instruments (Bel, Belsorp-miniII, Japan). Before measurement, the polymers were heated at 120 °C for 2 h. Standard Brunauer-Emmett-Teller (BET) and Barrett-Joyner-Halenda (BJH) were used for calculation of specific surface area, pore-volume, and average pore diameter. Fourier transform infrared spectra (4000 – 400 cm1) of MIPs and NIPs particles were recorded on a Bruker spectrometer (Perkin Elmer, USA).

Binding studies

Binding affinity of the imprinted and non-imprinted polymers was evaluated using a static adsorption experiment by separately mixing of 30 mg of polymer particles with various concentrations of BPA (0.1-2.5 mmol/L) in acetonitrile (CAN). The solution was shaken at 250 rpm for 3h at room temperature. After binding, the polymer particles were separated by centrifugation at 15000 rpm for 30 min. The free concentrations of BPA were determined by absorption at 278 nm. The adsorption capacity of MIPs and NIPs were determined by Equation (1) [27]:

$$Q = \frac{(C_0 - C_f)v}{m} \quad (1)$$

where C_0 (mmol/L) and C_f (mmol/L) are the initial and final concentrations of BPA, v (L) is the volume of solution, m(g) is the mass of the polymer, Q (μmol/g) is the amount of BPA. The removal efficiency was also calculated according to the following equation:

$$Removal\ efficiency\ (\%) = \frac{C_0 - C_e}{C_0} \times 100 \quad (2)$$

where, C_e is the equilibrium concentrations of BPA (mmol/L).

In dynamic adsorption experiments to study the reaction kinetics, 30 mg of MIP particles were mixed with 15 mL of acetonitrile solution with different concentrations of BPA (0.1-2.5 mmol/L). The solution was shaken at 250 rpm. The samples were taken from the solution at an interval of 30 min and the unbound BPA was measured by a UV-visible spectrophotometer at 278 nm.

The imprinting factor which shows the diagnostic characterization of MIPs and NIPs to the template molecules was determined according to Equation (3):

$$IF = \frac{Q_{MIP}}{Q_{NIP}} \quad (3)$$

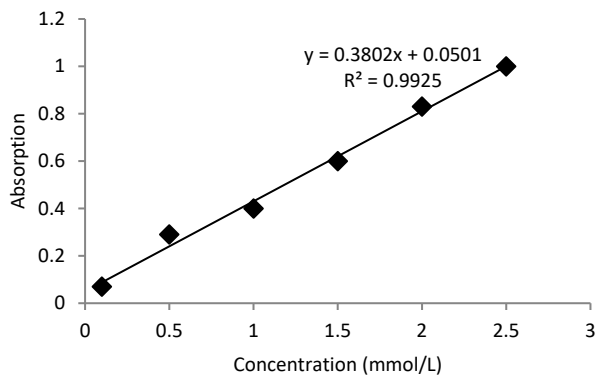

Fig. 1: Standard absorption plot for BPA

Isotherm study

Experimental data were fitted to the Langmuir, Freundlich, and Scatchard models for the determination of the isotherm parameters. Langmuir adsorption model assumes that each fixed number of homogenous sites can only adsorb on the molecule of the samples [28]. The Langmuir model can be applied as below:

$$Q_e = \frac{Q_{max} b C_e}{1 + b C_e} \quad (4)$$

where, Ce (mmol/L) is the equilibrium concentration of the BPA, Q_e (mmol/g) is the amount BPA per unit mass of adsorbent at equilibrium concentration, Q_{max} (mmol/g) is the maximum adsorption capacity, b is the adsorption equilibrium constant.

The non-homogenous and reversible adsorption of BPA on adsorbent can be described by Freundlich isotherm as Equation (5):

$$Q_e = k_F C_e^{1/n} \quad (5)$$

Where, n and K_F (mmol/g) are Freundlich constants.

The Scatchard plot analysis is applied to obtain further knowledge on the affinity of binding sites [29]. The experimental data were analyzed using the Scatchard equation as below:

$$\frac{Q_e}{C_e} = (Q_{max} - Q_e) K_d \quad (6)$$

where, K_d is the dissociation constant.

Kinetic study

Most of the adsorption process is related to time. Kinetic models describe the adsorption rate of adsorbate and its dependency on time. Kinetic models of pseudo-first order and pseudo-second-order were used to investigate BPA adsorption onto synthesized polymers.

The pseudo-first-order equation is stated in the linear form as below:

$$\ln(q_e - q_t) = lnq_e - K_1 t \quad (7)$$

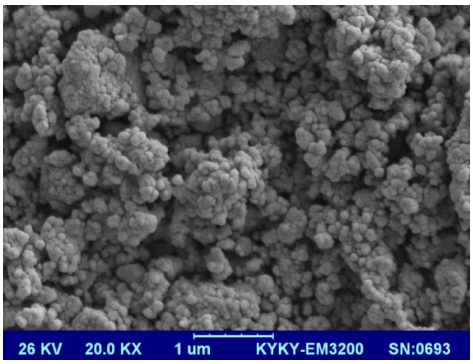

MIP-4

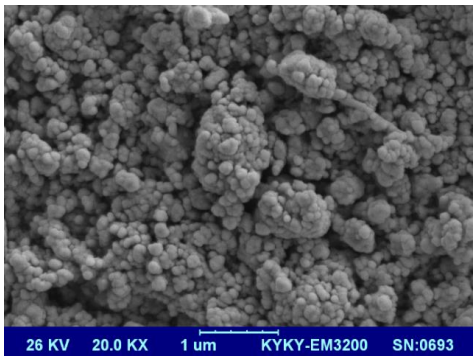

MIP-6

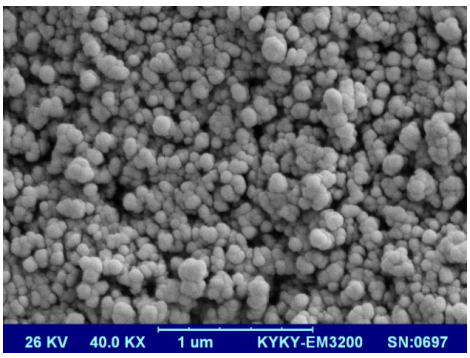

NIP-4

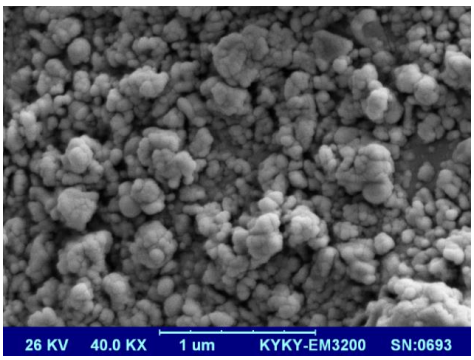

NIP-6

Fig. 2: SEM images of MIPs and NIPs

where, q_e and q_t are the amount of BPA adsorbed (mg/g) on the adsorbent at the equilibrium and at time t, respectively, and K_1 (1/min) is the rate of constant adsorption.

The (q_e) and (K_1) parameters can be calculated from the slope and intercept of the plot of $Ln(q_e-q_t)$ versus time. The pseudo-second-order equation is expressed as follow:

$$\frac{t}{q_t} = \frac{1}{k_2 q_e^2} + \frac{1}{q_e} t \quad (8)$$

where, k_2 is the rate constant of pseudo-second-order equation (μmol/mg min).

RESULT AND DISCUSSION

Characterization studies

Fig. 2 shows the surface morphology of MIPs and NIPs. Nanometer and spherical particles were achieved by precipitation polymerization. Since the addition of template to polymerization solution causes cavities formation in polymer network [30], the NIPs showed fairly regular and smooth surface rather than MIPs. Thus, the MIPs had a porous surface compared to NIPs due to the presence of BPA.

The FT-IR spectra of synthesized MIPs and NIPs are shown in Fig. 3. Similar characteristic peaks confirmed similarity in the structure of polymers. However, there are obvious differences between the IR spectra of the MIPs and NIPs. Absorption peaks at 3400 to 3500 cm^{-1} is related to stretching vibration of O-H. Bonds at 1730 cm^{-1} are linked to the stretching vibration of C=O of –COOH group of MAA. Furthermore, absorption peaks at 1380 to 1400 cm^{-1} and 1460 cm^{-1} are related to the bending vibration of CH_3 and CH_2 groups, respectively. The peak at 1640 cm^{-1} corresponded to the stretching vibration of C=C bonds.

The porosities of produced MIPs and NIPs were

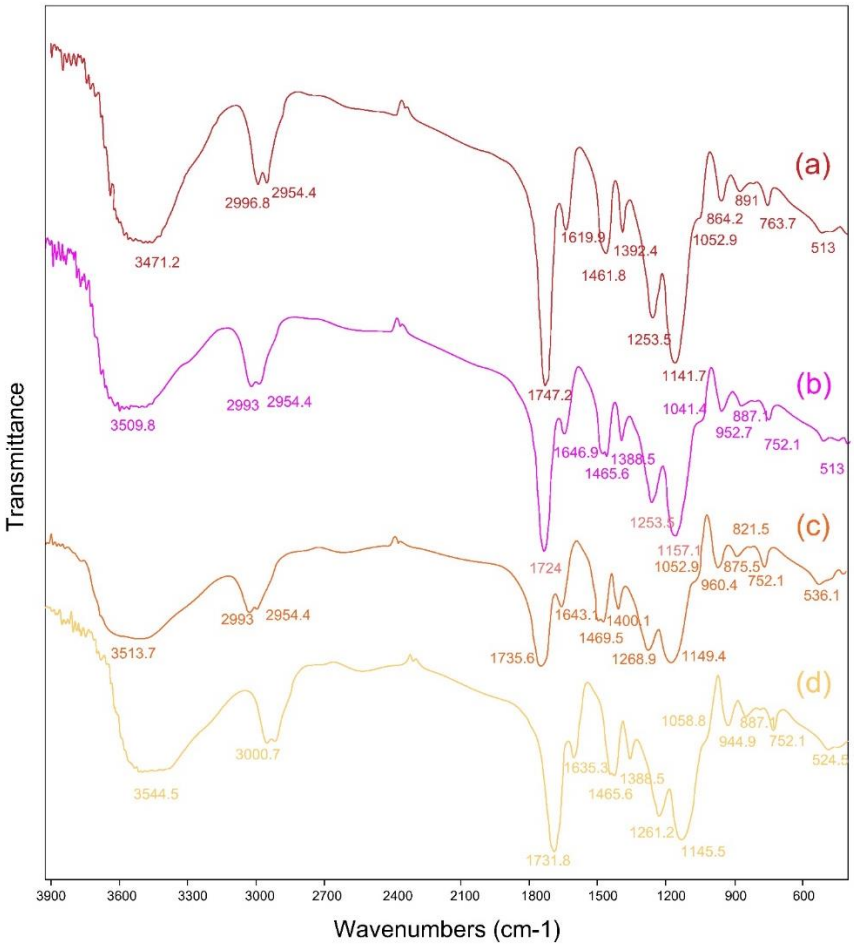

Fig. 3: FTIRs of (a) MIP-4, (b) MIP-6, (c) NIP-4 and (d) NIP-6

evaluated by the nitrogen adsorption-desorption experiment (Fig. 4). The results of the BET analysis are shown in Table 1. Pore volume, specific surface area, and average pore diameter of the MIPs are compared with the NIPs. Since the pore diameter of synthesized polymers is in the range of 2 to 50 nm, they are placed in the mesoporous category. The specific surface area of MIPs is larger than that of the corresponding NIPs, which may result due to the presence of cavities on MIPs. This may be owing to the presence template molecule, such that after its removal from the polymer, it left particles of the MIP with a higher surface area. It indicates the higher accessibility of imprinted cavities and so higher adsorption capacity of MIPs to BPA than that of the corresponding NIP due to imprinting effect. Moreover, a decrease in particle size increased their specific surface area and pore volume. In Fig. 4, at low relative pressure (P/P_0), the amount of adsorption increased with a uniform gradient which is related to the adsorption of nitrogen molecules on the internal surface of the mesoporous polymer. As this ratio of (P/P_0) increased, the adsorption increased rapidly due to the filling of mesoporous polymer with gas molecules and their density on the surface.

The adsorption capacity of MIPs and NIPs and isotherm models

Fig. 5 shows the effect of various initial concentrations of BPA (0.1 to 2.5 mmol/L) onto the adsorption capacity and removal efficiency of MIPs and NIPs. The adsorption capacity (amount of BPA adsorbed per unit mass of polymers) increased with an increase in the initial concentration of BPA. At low concentrations, most of the active sites

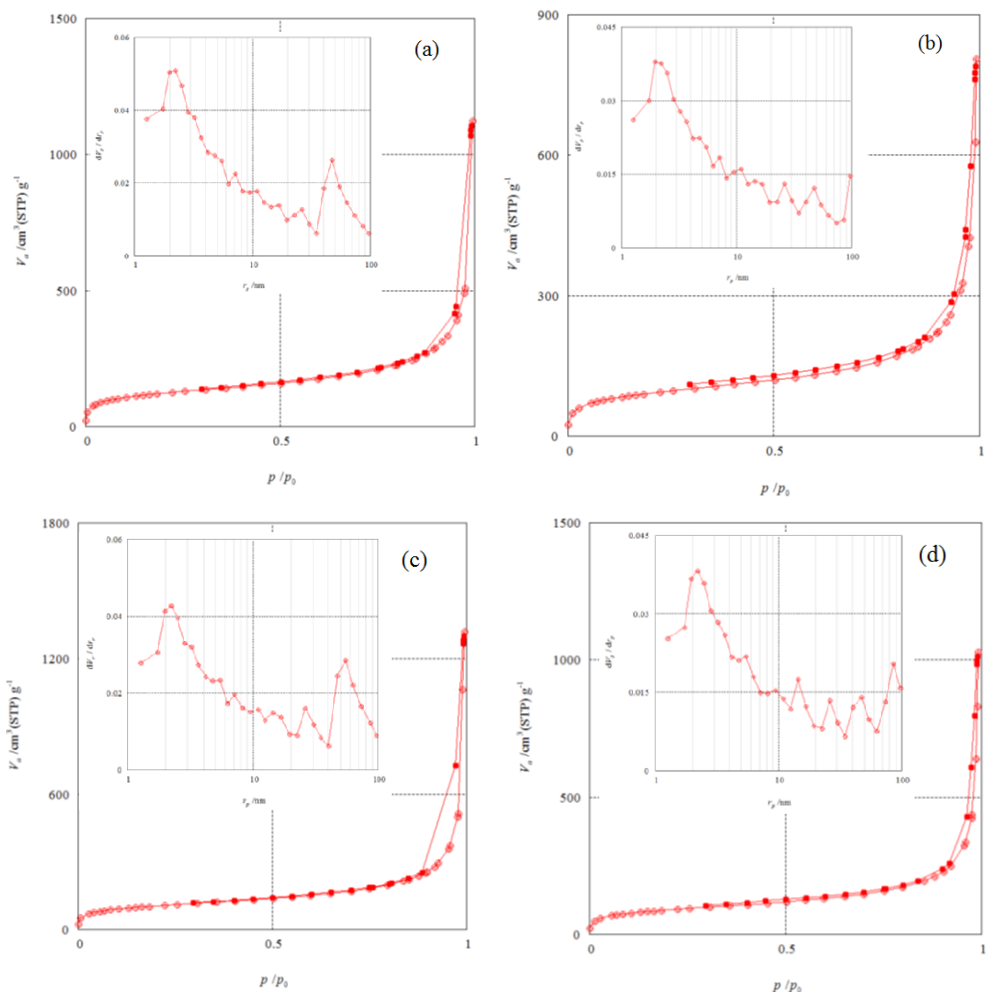

Fig. 4: Nitrogen adsorption-desorption isotherm of (a) MIP-4, (b) MIP-6, (c) NIP-4 and (d) NIP-6. (The BJH plot are given in inset)

Table 1. Results of BET analysis for polymers

Polymer	Specific surface area (m^2/g)	Pore volume (m^3/g)	Average pore diameter (nm)
MIP-6	439.60	1.5515	13.590
MIP-4	378.65	1.1177	14.118
NIP-6	328.99	1.7014	17.738
NIP-4	326.21	1.4465	17.974

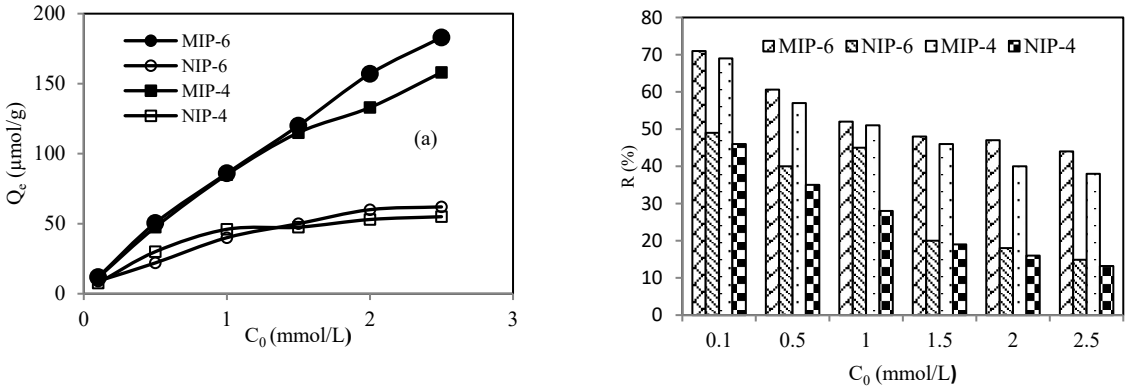

Fig. 5: The effect of initial concentrations of BPA onto (a) adsorption capacity and (b) removal efficiency of MIPs and NIPs

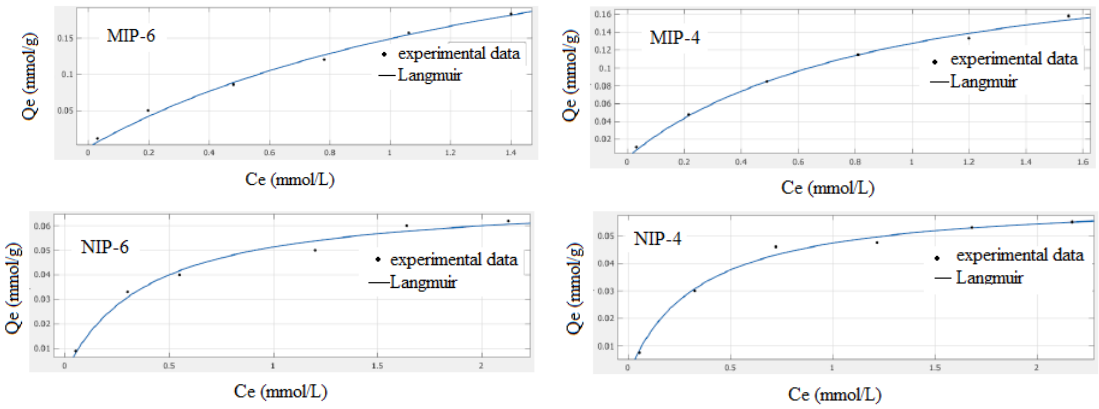

Fig. 6: Langmuir adsorption isotherm of BPA onto polymers

remained unsaturated and the binding capacity was low. However, an increase in the initial concentration of BPA resulted in mass transfer enhancement and adsorption capacity. As shown in Fig. 5, MIPs polymer has a greater binding capacity than that of NIPs. The highest binding capacity was obtained for MIP-6 with a value of 183 µmol/g. Also, due to the reduction in active sites of adsorbent because of increasing in BPA concentration, the removal efficiency decreased.

Langmuir, Freundlich, and Scatchard isotherm models were used to evaluate the interaction between BPA molecules and synthesized polymers. Fig. 6 and Table 2 show the Langmuir isotherm plots and model constants, respectively. The results indicated that the Langmuir model is a suitable isotherm for interpreting the adsorption data obtained for adsorption of BPA onto polymers due to high correlation coefficients. The maximum adsorption capacity achieved for MIP-6 (400.1 µmol/g) was higher than that obtained for MIP-4 (245.5 µmol/g).

Freundlich isotherm plot is shown in Fig. 7. The constants and correlation coefficient (R^2) are

Table 2: Isotherm parameters for BPA adsorption

Models	Parameters	MIP-6	MIP-4	NIP-6	NIP-4
Langmuir	Q_m (μmol/g)	400.1	245.5	72.04	63.79
	b (L/mmol)	0.593	1.081	2.49	2.875
	R^2	0.9924	0.9958	0.9844	0.9909
Freundlich	K_f(mmol/g)	0.1462	0.1233	0.0477	0.0438
	n (L/mmol)	1.448	1.722	2.52	2.663
	R^2	0.9977	0.9935	0.9693	0.928

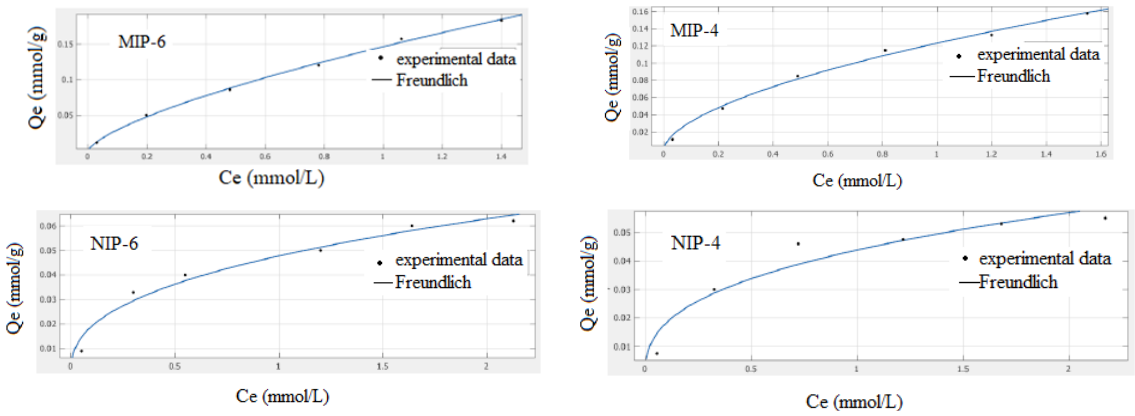

Fig. 7: Freundlich adsorption isotherm of BPA onto polymers

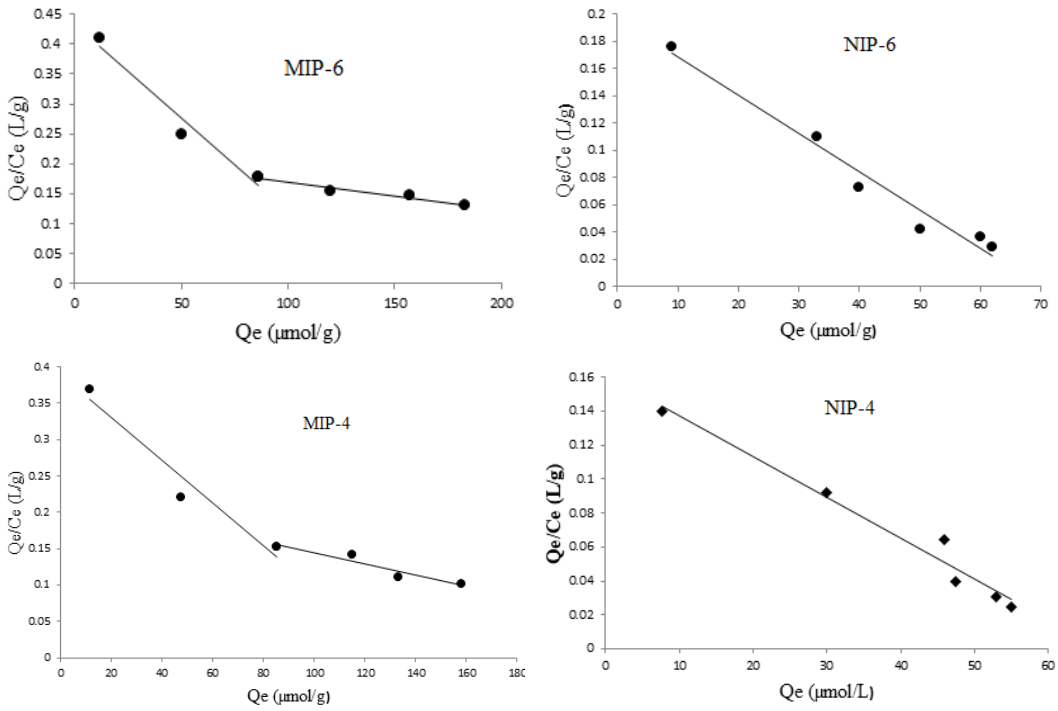

Fig. 8: Scatchard plot analysis of the BPA binding onto the polymers

Table 3. Scatchard parameters for MIPs

Polymers	Adsorption capacity at high-affinity binding sites Q_{max} (μmol/g)	Adsorption capacity at low-affinity binding sites Q_{max} (μmol/g)	Dissociation constant at high-affinity binding sites K_d (μmol/L)	Dissociation constant at low-affinity binding sites K_d (μmol/L)
MIP-6	139.87	430	322.58	2000
MIP-4	133.81	274.87	344	1250

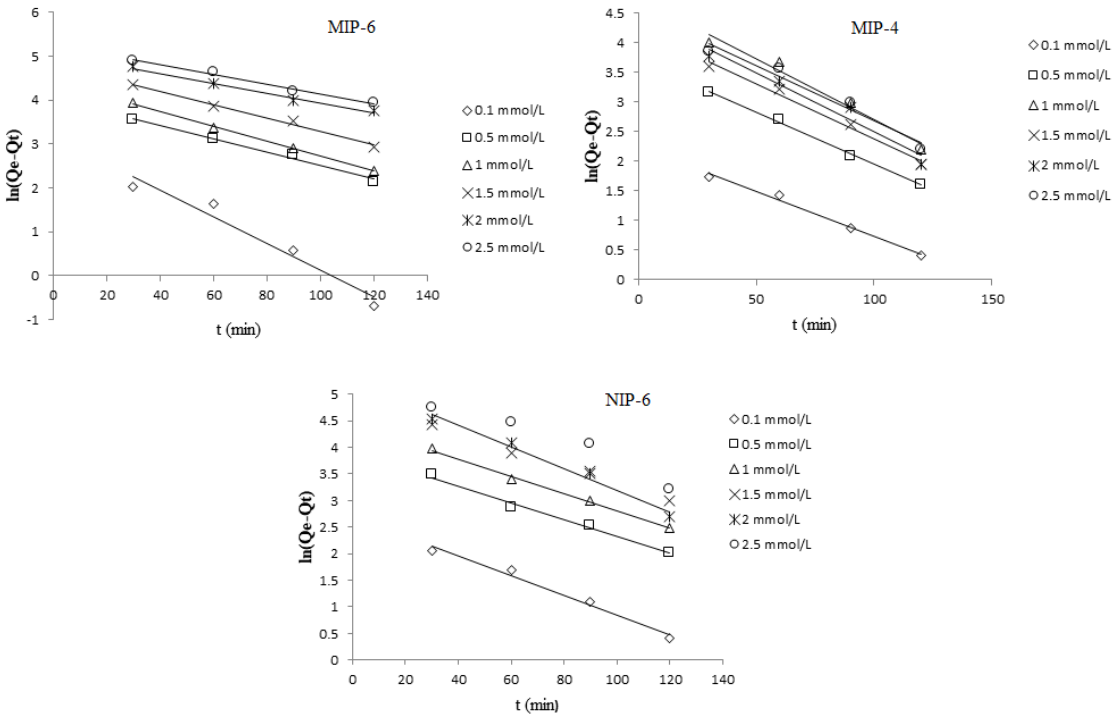

Fig. 9: Pseudo-first-order plot of BPA onto MIPs and NIPs

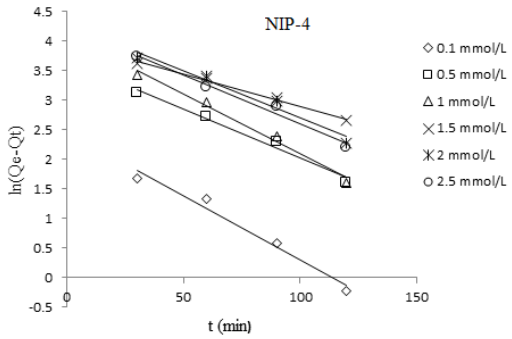

Fig. 10: Pseudo-second-order plot of BPA onto MIPs and NIPs

illustrated in Table 2. Results show that adsorption data were in good agreement with Freundlich isotherm with high correlation coefficients. The n values obtained for MIPs and NIPs were between 1 to 10 indicating good surface adsorption and suitability of the adsorption of BPA onto the polymers. The constant value of b and K_F obtained for MIPs is smaller than that of NIPs which showed that BPA had more affinity to synthesized MIPs compared to NIPs.

Table 4. Kinetic parameters for BPA adsorption

Polymer	The initial concentration of BPA	q_e(exp) (μmol/g)	Pseudo-first order			Pseudo-second order		
			q_e(cal) (μmol/g)	K_1(1/min)	R^2	q_e(cal) (μmol/g)	K_2	R^2
MIP-6	0.1	11.8	24.24	0.0306	0.9543	23.42	3×10^{-4}	0.937
	0.5	50.5	55.98	0.0152	0.9892	103.09	5.84×10^{-5}	0.969
	1	86	83	0.017	0.9987	129.87	9.58×10^{-5}	0.990
	1.5	120	123	0.0153	0.9885	208.33	4.036×10^{-5}	0.970
	2	157	158.38	0.0112	0.9891	526.31	5.34×10^{-6}	0.860
	2.5	183	190.56	0.0111	0.9924	526.31	5.95×10^{-6}	0.810
MIP-4	0.1	11.5	14.9	0.0185	0.9807	25.25	0.0002	0.9787
	0.5	47.5	49.66	0.0158	0.9880	90	8×10^{-5}	0.9342
	1	85	83.72	0.0162	0.9959	135.13	7.8×10^{-5}	0.9829
	1.5	115	129.67	0.0153	0.9924	277.77	1.657×10^{-5}	0.9003
	2	133	186.23	0.0203	0.9824	312.5	1.61×10^{-5}	0.9880
	2.5	158	219.2	0.0168	0.9391	625	3.54×10^{-6}	0.8330
NIP-6	0.1	9	9.511	0.0152	0.9887	16.103	4.82×10^{-4}	0.9477
	0.5	35	40.93	0.0176	0.9961	82.64	5.41×10^{-5}	0.9392
	1	75	115.58	0.0204	0.9708	270.27	9.76×10^{-6}	0.8549
	1.5	50	69.75	0.0186	0.9866	178.57	1.51×10^{-5}	0.9331
	2	60	88.58	0.0198	0.9546	185.18	1.76×10^{-5}	0.9521
	2.5	62	93.45	0.0185	0.9587	270.27	7.46×10^{-5}	0.9371
NIP-4	0.1	7.6	11.763	0.0216	0.9729	21.321	1.8×10^{-4}	0.9271
	0.5	30	39.98	0.0164	0.9803	107.53	2.4×10^{-5}	0.9423
	1	46	60.8	0.0210	0.9863	93.46	6.96×10^{-5}	0.9965
	1.5	47.5	53.76	0.108	0.912	476.19	1.42×10^{-6}	0.9982
	2	53	72.56	0.0159	0.9641	454.54	1.93×10^{-6}	0.9654
	2.5	55	69.75	0.0164	0.9792	217.39	1.05×10^{-5}	0.9100

Table 5. Imprinting factor for synthesized polymers at various BPA concentrations

BPA concentration (mmol/L)	α (1:4:20)	α (1:6:30)
0.1	1.151	1.456
0.5	1. 53	1.53
1	1.85	2.15
1.5	2.42	2.4
2	2.5	2.61
2.5	2.87	2.95

The Scatchard analysis curves of MIPs and NIPs are illustrated in Fig. 8. As shown in Fig. 8, the nonlinear relationship between Qe/Ce and Qe was achieved. It indicated that the interaction sites between the template molecules and the functional monomers were not uniform during the synthesis of the MIPs for both high (left portion of the Fig.8) and low (right portion of the Fig.8)-affinity binding sites. Besides, all template molecule bonds did not participate in the polymerization reaction. The obtained result for K_a and Q_{max} is shown in Table 3. For NIP-6 and NIP-4, the K_a was calculated to be 357.14 and 416.66 μmol/L, respectively and the corresponding value of Q_{max} was 70.36 and 67.165 μmol/g, respectively.

Adsorption kinetics

Figs. 9 and 10 show the pseudo-first-order and pseudo-second-order plots for BPA adsorption onto polymers, respectively. Kinetic parameters are presented in Table 4. As seen in Table 4, the higher regression coefficients (R^2) were obtained for data fitting to the first-order kinetic model for NIPs and MIPs. Besides, the calculated adsorption capacity ($q_{eq,cal}$) achieved from the pseudo-first-order model agreed with the experimental adsorption capacity ($q_{e,exp}$). Thus, the pseudo-first-order model could describe the adsorption of BPA onto synthesized NIPs and MIPs well. On the other hand, the binding kinetics obtained for MIPs are improved because of higher surface-area-to-volume ratios and more

accessibility of imprinted cavities by BPA.

Imprinting factor

The imprinting factors for synthesized polymers with two molecular ratios of 1:4:20 and 1:6:30 polymers are presented in Table 5. The imprinting factor at high BPA concentrations increased in contrast to low BPA concentrations.

CONCLUSION

In this work, nano-sized MIPs were synthesized by precipitation polymerization, allowing BPA removal from water solution. The produced nanoparticles have a high surface-area-to-volume ratio; consequently, binding performance is suitable due to easier access of imprinted pores by the template. The effect of various factors such as the amount of the molecular ratio of template: functional monomer: cross-linker and initial concentrations of BPA onto adsorption capacity and removal efficiency of MIPs and NIPs were evaluated. The 1:6:30 ratio showed better removal of BPA rather than a 1:4:20 ratio. Moreover, the results indicated the nano-spherical morphology of MIPs. The adsorption isotherm and kinetic models were used to determine the mechanism and binding properties of polymers. The adsorption kinetics were in good agreement with the pseudo-first-order model. The results depicted that the synthesized MIP could be considered as an appropriate adsorbent for BPA removal.

ACKNOWLEDGMENTS

The authors are grateful to the Islamic Azad University of Amol Branch (Amol, Iran) for its support to do this research.

CONFLICT OF INTEREST

There are no conflicts to declare.

REFERENCES

1. Zhou H, Xu Y, Tong H, Liu Y, Han F, Yan X, et al. Direct synthesis of surface molecularly imprinted polymers based on vinyl-SiO2nanospheres for recognition of bisphenol A. Journal of Applied Polymer Science. 2012;128(6):3846-52.
2. Yin J, Meng Z, Zhu Y, Song M, Wang H. Dummy molecularly imprinted polymer for selective screening of trace bisphenols in river water. Anal Methods. 2011;3(1):173-80.
3. Yan H, Liu S, Gao M, Sun N. Ionic liquids modified dummy molecularly imprinted microspheres as solid phase extraction materials for the determination of clenbuterol and clorprenaline in urine. Journal of Chromatography A. 2013;1294:10-6.
4. Curcio P, Zandanel C, Wagner A, Mioskowski C, Baati R. Semi-Covalent Surface Molecular Imprinting of Polymers by One-Stage Mini-emulsion Polymerization: Glucopyranoside as a Model Analyte. Macromolecular Bioscience. 2009;9(6):596-604.
5. Wang Y, Liu Q, Rong F, Fu D. A facile method for grafting of bisphenol A imprinted polymer shells onto poly(divinylbenzene) microspheres through precipitation polymerization. Applied Surface Science. 2011;257(15):6704-10.
6. Luliński P, Dana M, Maciejewska D. Synthesis and characterization of 3,4-dihydroxyphenylacetic acid imprinted polymers. Polymer International. 2011;61(4):631-8.
7. Abouzarzadeh A, Forouzani M, Jahanshahi M, Bahramifar N. Synthesis and evaluation of uniformly sized nalidixic acid-imprinted nanospheres based on precipitation polymerization method for analytical and biomedical applications. Journal of Molecular Recognition. 2012;25(7):404-13.
8. Yoshimatsu K, Yamazaki T, Chronakis IS, Ye L. Influence of template/functional monomer/cross-linking monomer ratio on particle size and binding properties of molecularly imprinted nanoparticles. Journal of Applied Polymer Science. 2011;124(2):1249-55.
9. Beyki T, Asadollahzadeh MJ. Selective removal of dicamba from aqueous samples using molecularly imprinted polymer nanospheres. J. Water Environ. Nanotechnol. 2016;1(1):19-25.
10. Yoshimatsu K, Reimhult K, Krozer A, Mosbach K, Sode K, Ye L. Corrigendum to "Uniform molecularly imprinted microspheres and nanoparticles prepared by precipitation polymerization: The control of particle size suitable for different analytical applications" [Anal. Chim. Acta 584 (2007) 112–121]. Analytica Chimica Acta. 2010;657(2):215.
11. Refaat D, Aggour MG, Farghali AA, Mahajan R, Wiklander JG, Nicholls IA, et al. Strategies for Molecular Imprinting and the Evolution of MIP Nanoparticles as Plastic Antibodies—Synthesis and Applications. International Journal of Molecular Sciences. 2019;20(24):6304.
12. Soleimani M, Ghaderi S, Afshar MG, Soleimani S. Synthesis of molecularly imprinted polymer as a sorbent for solid phase extraction of bovine albumin from whey, milk, urine and serum. Microchemical Journal. 2012;100:1-7.
13. Maragou NC, Thomaidis NS, Theodoridis GA, Lampi EN, Koupparis MA. Determination of bisphenol A in canned food by microwave assisted extraction, molecularly imprinted polymer-solid phase extraction and liquid chromatography-mass spectrometry. Journal of Chromatography B. 2020;1137:121938.
14. Moreira FTC, Sales MGF. Biomimetic sensors of molecularly-imprinted polymers for chlorpromazine determination. Materials Science and Engineering: C. 2011;31(5):1121-8.
15. Alenazi N, Manthorpe J, Lai E. Selectivity Enhancement in Molecularly Imprinted Polymers for Binding of Bisphenol A. Sensors. 2016;16(10):1697.
16. Yuan Y, Liu Y, Teng W, Tan J, Liang Y, Tang Y. Preparation of core-shell magnetic molecular imprinted polymer with binary monomer for the fast and selective extraction of bisphenol A from milk. Journal of Chromatography A. 2016;1462:2-7.
17. Zaidi SA. Molecular imprinting: A useful approach for drug delivery. Materials Science for Energy Technologies. 2020;3:72-7.
18. Tarannum N, Hendrickson OD, Khatoon S, Zherdev AV,

Dzantiev BB. Molecularly imprinted polymers as receptors for assays of antibiotics. Critical Reviews in Analytical Chemistry. 2019:1-20.
19. Jurek A, Leitner E. Analytical determination of bisphenol A (BPA) and bisphenol analogues in paper products by LC-MS/MS. Food Additives & Contaminants: Part A. 2018;35(11):2256-69.
20. Zhang J, Li X, Zhou L, Wang L, Zhou Q, Huang X. Analysis of effects of a new environmental pollutant, bisphenol A, on antioxidant systems in soybean roots at different growth stages. Scientific Reports. 2016;6(1).
21. Caballero-Casero N, Lunar L, Rubio S. Analytical methods for the determination of mixtures of bisphenols and derivatives in human and environmental exposure sources and biological fluids. A review. Analytica Chimica Acta. 2016;908:22-53.
22. Huang YQ, Wong CKC, Zheng JS, Bouwman H, Barra R, Wahlström B, et al. Bisphenol A (BPA) in China: A review of sources, environmental levels, and potential human health impacts. Environment International. 2012;42:91-9.
23. Park C, Song H, Choi J, Sim S, Kojima H, Park J, et al. The mixture effects of bisphenol derivatives on estrogen receptor and androgen receptor. Environmental Pollution. 2020;260:114036.
24. Hiratsuka Y, Funaya N, Matsunaga H, Haginaka J. Preparation of magnetic molecularly imprinted polymers for bisphenol A and its analogues and their application to the assay of bisphenol A in river water. Journal of Pharmaceutical and Biomedical Analysis. 2013;75:180-5.
25. Alexiadou DK, Maragou NC, Thomaidis NS, Theodoridis GA, Koupparis MA. Molecularly imprinted polymers for bisphenol A for HPLC and SPE from water and milk. Journal of Separation Science. 2008;31(12):2272-82.
26. Karaman Ersoy Ş, Tütem E, Sözgen Başkan K, Apak R, Nergiz C. Preparation, characterization and usage of molecularly imprinted polymer for the isolation of quercetin from hydrolyzed nettle extract. Journal of Chromatography B. 2016;1017-1018:89-100.
27. Sun X, Wang J, Li Y, Jin J, Zhang B, Shah SM, et al. Highly selective dummy molecularly imprinted polymer as a solid-phase extraction sorbent for five bisphenols in tap and river water. Journal of Chromatography A. 2014;1343:33-41.
28. Langmuir I. THE ADSORPTION OF GASES ON PLANE SURFACES OF GLASS, MICA AND PLATINUM. Journal of the American Chemical Society. 1918;40(9):1361-403.
29. Scatchard G. THE ATTRACTIONS OF PROTEINS FOR SMALL MOLECULES AND IONS. Annals of the New York Academy of Sciences. 1949;51(4):660-72.
30. Bayramoglu G, Arica MY, Liman G, Celikbicak O, Salih B. Removal of bisphenol A from aqueous medium using molecularly surface imprinted microbeads. Chemosphere. 2016;150:275-84.